

An Improved High-Degree Cubature Particle Filter and its Application in Bearing-only Tracking

Yanqi Niu¹, Dandan Zhu¹ and Yaan Li¹

Received: 21 October 2024 / Accepted: 17 April 2025
© Harbin Engineering University and Springer-Verlag GmbH Germany, part of Springer Nature 2026

Abstract

In this study, a fifth-degree cubature particle filter (5CPF) is proposed to address the limited estimation accuracy in traditional particle filter algorithms for bearings-only tracking (BOT). This algorithm calculates the recommended density function by introducing a fifth-degree cubature Kalman filter algorithm to guide particle sampling, which effectively alleviates the problem of particle degradation and significantly improves the estimation accuracy of the filter. However, the 5CPF algorithm exhibits high computational complexity, particularly in scenarios with a large number of particles. Therefore, we propose the extended Kalman filter (EKF)-5CPF algorithm, which employs an EKF to replace the time update step for each particle in the 5CPF. This enhances the algorithm's real-time capability while maintaining the high precision advantage of the 5CPF algorithm. In addition, we construct bearing-only dual-station and single-motion station target tracking systems, and the filtering performances of 5CPF and EKF-5CPF algorithms under different conditions are analyzed. The results show that both the 5CPF algorithm and EKF-5CPF have strong robustness and can adapt to different noise environments. Furthermore, both algorithms significantly outperform traditional nonlinear filtering algorithms in terms of convergence speed, tracking accuracy, and overall stability.

Keywords Nonlinear filtering; Fifth-degree cubature particle filter; EKF-5CPF; Bearings-only target motion analysis

1 Introduction

Bearings-only target tracking (BOT) is a classic passive tracking method that does not entail the sonar system actively transmitting and receiving sound waves to detect a target (Gao et al., 2010; Nardone et al., 1984). Instead, it acquires azimuthal measurement information through passive signal reception, thereby estimating a target's distance and motion status (Farina, 1999; Xu and Wang, 2006). It advantageously has high concealment in actual combat and can implement sudden strikes on targets, constituting an important part of tracking defense systems (Pillon et al., 2016).

In BOT motion analysis, nonlinear filtering algorithms have always been the focus and difficulty of scientific research (Badriasl et al., 2020), such as extended Kalman filter (EKF) (Weiss and Moore, 1980), unscented Kalman filter (UKF) (Divya et al., 2021; Kumar et al., 2016), and particle filter (PF) (Arulampalam et al., 2002). However, UKF and EKF algorithms can only be used in Gaussian noise systems, which has certain limitations. Meanwhile, although PF is not limited by any noise model and system model, it is generally affected by particle degradation. This problem causes the algorithm to spend a lot of time on invalid calculations during execution, affecting filtering time and accuracy (Arulampalam and Ristic, 2000).

In recent years, nonlinear filtering algorithms have been rapidly developed. For instance, the cubature Kalman filter (CKF) replaces the linearization process by selecting cubature points following a spherical-radial rule (Arasaratnam and Haykin, 2009). However, although CKF demonstrates greater stability than the traditional UKF, its accuracy is comparable to that of UKF or may even be inferior. Jia et al. (2012) proposed an arbitrary-degree CKF with improved accuracy compared with those of traditional UKF and CKF, which employed the spherical-radial cubature rule to determine cubature points and applied it in BOT. However, as the number of cubature points increased, the calculation amount and time of the algorithm also increased signifi-

Article Highlights

- A 5CPF algorithm is proposed for a bearings-only target tracking system.
- Combining the EKF with the 5CPF algorithm enhances the real-time performance of the system.
- Models of dual observation stations and a single motion observation station are established, and the performances of the 5CPF and EKF-5CPF algorithms are evaluated.

✉ Yaan Li
liyaan@nwpu.edu.cn

¹ School of Marine Science and Technology, Northwestern Polytechnical University, Xi'an 710072, China

cantly. Meanwhile, Wang et al. (2014) introduced a novel CKF utilizing a spherical single-channel criterion. Herein, the spherical integral was computed using the moment matching technique, which further improved the accuracy and efficiency of the traditional CKF algorithm. Zhu et al. (2020) proposed the adaptively robust square-root cubature Kalman filter (ARSRCKF) algorithm based on time-varying noise covariance to solve the problem where the CKF algorithm easily loses the non-negativity of the error Q and R in the time-varying noise system, which results in the filter diverging. The ARSRCKF algorithm always maintained positive definite or semipositive definite Q and R throughout the filtering process. Kulikova and Kulikov (2021) proposed the EKF-5CKF algorithm by combining the EKF algorithm and the fifth-degree CKF (5CKF) algorithm, which reduced the computational time of the 5CKF algorithm. Mu et al. (2024) proposed the adaptive fractional gain-based interpolatory cubature Kalman filter, which reduced the computational time of the 5CKF algorithm. However, it required large amounts of calculation in high-dimensional systems, and the filtering performance was poor and sensitive to measurement noise when the observed value was not accurate.

The emergence of PF can be traced back to the 1950s (Arulampalam et al., 2002). The Monte Carlo method of sequential importance sampling was proposed, which approximated probability distribution through discrete proposal distribution (Hammersley and Morton, 1954). However, it had high computational complexity and degradation problems. The main solution was to improve the proposal density function and use a resampling algorithm. Unscented PF (UPF) (van der Merwe et al., 2000) and Gaussian PF (GPF) (Kotecha and Djuric, 2003) solved the above problems to a certain extent by adopting appropriate suggested density distribution functions. However, UPF may have matrix singularity problems in practice, leading to its inability to work. Meanwhile, GPF alleviates the problem of particle scarcity, but it is not suitable for some nonlinear systems that cannot be approximated by Gaussian distribution. Havangi (2018) proposed the $H\infty$ algorithm by combining the UKF and the particle swarm optimization (PSO) algorithm. It used the PSO to optimize particles, realized the estimation of the target state, and proved its excellent performance in target tracking. Li et al. (2015) compared and analyzed the application of different resampling algorithms in particle filtering and found a difference in calculation time but no significant difference in estimation accuracy. Zhang et al. (2021) proposed a resampling strategy called the adaptive Metropolis-Hastings, which performed Gaussian mutation on low-weight particles. Compared with traditional methods, it increases the diversity of particles. However, this resampling method changes the original particle set; thus, the covariance matrix of the new particles cannot be calculated, which is not suitable for extended PF (EPF),

UPF, and other algorithms. With the progress of science and technology and the complexity of the current marine environment, nonlinear filters have increased performance requirements (Li and Zhao, 2019; Shen et al., 2025, 2024a, 2024b, 2024c).

Given the high precision and high real-time requirements of target tracking in current military operations, this paper first combines 5CKF with PF and proposes a new fifth-degree cubature PF (5CPF) algorithm. Through multiple tests in different simulation environments, the tracking effect of the 5CPF algorithm is analyzed in detail. In addition, the EKF algorithm is applied to 5CPF by leveraging its low calculation costs. Thus, the EKF-5CPF algorithm is proposed, which maintains the high-precision advantages of the 5CPF algorithm while reducing the calculation time, which is of great significance in practical applications.

2 Cubature kalman filter

2.1 Third-degree cubature Kalman filter

The CKF algorithm employs a third-degree spherical-radial cubature rule to address the filtering challenges of high-dimensional systems. By selecting a collection of cubature points in proximity to the current target state and iteratively updating them to predict the target state, the process can be outlined as follows:

- 1) Initialization parameters: $X_0, P_0, R,$ and $Q.$
- 2) Calculate the set of cubature points:

$$\zeta_i = \begin{cases} \sqrt{n} [1], & i = 1, 2, \dots, n \\ -\sqrt{n} [1], & i = n + 1, n + 2, \dots, 2n \end{cases} \quad (1)$$

$$\omega_i = \frac{1}{2n}, \quad i = 1, 2, \dots, 2n \quad (2)$$

$$S_k = \text{chol}(P_k)^T \quad (3)$$

$$X_{i,k} = S_k \zeta_i + \hat{X}_k, \quad i = 1, 2, \dots, 2n \quad (4)$$

In the above formulas, ζ_i is the i -th cubature point, P_k is the error matrix, $[1]$ is the unit matrix, and ω_i is the weight of each cubature point; The dimension of the system state is $n.$

- 3) State prediction:

$$X_{i,k+1|k} = f(X_{i,k}) \quad (5)$$

$$\hat{X}_{k+1|k} = \frac{1}{2n} \sum_{i=1}^{2n} X_{i,k+1|k} \quad (6)$$

$$P_{k+1|k} = \frac{1}{2n} \sum_{i=1}^{2n} X_{i,k+1|k} (X_{i,k+1|k})^T - \hat{X}_{k+1|k} (\hat{X}_{k+1|k})^T + Q_k \tag{7}$$

4) Measurement prediction:

$$Z_{k+1|k}^i = h(X_{i,k+1|k}) \tag{8}$$

$$\hat{Z}_{k+1|k} = \frac{1}{2n} \sum_{i=1}^{2n} Z_{k+1|k}^i \tag{9}$$

5) Covariance update:

$$S_{k+1|k} = \text{chol}(P_{k+1|k})^T \tag{10}$$

$$\hat{X}_{i,k+1|k} = \hat{X}_{k+1|k} + S_{k+1|k} \zeta_i \tag{11}$$

$$P_{Y,k+1|k} = \frac{1}{2n} \sum_{i=1}^{2n} (Z_{k+1|k}^i - \hat{Z}_{k+1|k}) (Z_{k+1|k}^i - \hat{Z}_{k+1|k})^T + R_k \tag{12}$$

$$P_{XY,k+1|k} = \frac{1}{2n} \sum_{i=1}^{2n} (\hat{X}_{i,k+1|k} - \hat{X}_{k+1|k}) (Z_{k+1|k}^i - \hat{Z}_{k+1|k})^T \tag{13}$$

6) Kalman gain:

$$K_k = P_{XY,k+1|k} (P_{Y,k+1|k})^{-1} \tag{14}$$

7) Target state update:

$$\hat{X}_k = \hat{X}_{k+1|k} + K_k (Z_k - \hat{Z}_{k+1|k}) \tag{15}$$

$$P_k = P_{k+1|k} - K_k P_{Y,k+1|k} K_k^T \tag{16}$$

2.2 Fifth-degree cubature kalman filter

The fifth-degree cubature Kalman filter uses more cubature points than CKF, resulting in higher stability and filtering accuracy in theory. However, its high accuracy is obtained at the cost of longer calculation time. The process

of the 5CKF algorithm is similar to that of CKF, but there are differences in the selection rules and weight calculation of the cubature points. For the fifth-degree spherical integral,

$$I_{U_n,5}(g_s) = \sum_{|p|=2} \omega_p G\{u_p\} \tag{17}$$

$$\omega_p \triangleq I_{U_n} \left(\prod_{i=1}^n \prod_{j=0}^{p_i-1} \frac{\delta_i^2 - u_j^2}{u_{p_i}^2 - u_j^2} \right) \tag{18}$$

$$G\{u_p\} \triangleq 2^{-c(u_p)} \sum_v g_s(v_1 u_{p_1}, v_2 u_{p_2}, \dots, v_n u_{p_n}) \tag{19}$$

In the above formulas, I_{U_n} denotes the spherical integral, p_i is a nonnegative integer, and $|P| = \sum_{i=1}^n p_i = 2$, where $u_{p_i} = \sqrt{p_i/2}$, $v_i = \pm 1$. Therefore, there are three different $u_{p_i} \left(0, \frac{1}{2}, 1\right)$ values, and the fifth-degree spherical rule can be obtained as follows (Singh and Bhaumik, 2015; Jia et al., 2013):

$$\int_{U_{n,5}} g_s(s) d\sigma(s) = \omega_{s,1} \sum_{j=1}^{n(n-1)/2} (g_s(\delta_1^{(j)}) + g_s(-\delta_1^{(j)}) + g_s(\delta_2^{(j)}) + g_s(-\delta_2^{(j)})) + \omega_{s,2} \sum_{j=1}^n (g_s(\rho_j) + g_s(-\rho_j)) \tag{20}$$

$$\begin{cases} \delta_1^{(j)} = \sqrt{\frac{1}{2}} (\rho_k + \rho_l), k < l, k, l = 1, 2, \dots, n \\ \delta_2^{(j)} = \sqrt{\frac{1}{2}} (\rho_k - \rho_l), k < l, k, l = 1, 2, \dots, n \end{cases} \tag{21}$$

where n is the dimension of the state equation, and ρ_j is an n -dimensional column vector whose j -th row values are all 1 and the remaining values are all 0.

$$\begin{cases} \gamma_0 = 0, \omega_0 = \frac{2}{n+2} \\ \gamma_i = \sqrt{n+2} \delta_1^{(j)}, \omega_i = \frac{1}{(n+2)^2}, i = 1, 2, \dots, N \\ \gamma_i = -\sqrt{n+2} \delta_1^{(j)}, \omega_i = \frac{1}{(n+2)^2}, i = 1, 2, \dots, N \\ \gamma_i = -\sqrt{n+2} \delta_2^{(j)}, \omega_i = \frac{1}{(n+2)^2}, i = 2N+1, \dots, 3N \\ \gamma_i = \sqrt{n+2} \delta_2^{(j)}, \omega_i = \frac{1}{(n+2)^2}, i = 3N+1, \dots, 4N \\ \gamma_i = \sqrt{n+2} \rho_j, \omega_i = \frac{4-n}{2(n+2)^2}, i = 4N+1, \dots, 4N+n; j = i-4N \\ \gamma_i = -\sqrt{n+2} \rho_j, \omega_i = \frac{4-n}{2(n+2)^2}, i = 4N+n+1, \dots, 2n^2; j = i-4N-n \end{cases} \tag{22}$$

where $N = \frac{n(n-1)}{2}$ and ω_i denotes the weight of the i -th cubature point. Taking a uniform linear moving target as an example, the third-degree CKF generally selects eight cubature points near each target state prediction, whereas 5CKF selects approximately 33 cubature points, which enhances the efficiency of the algorithm but increases the operation time.

3 Improved cubature PF

Given that the filtering performance of the 5CKF algorithm surpasses that of the CKF algorithm, we integrate the 5CKF algorithm with the PF algorithm to introduce both the 5CPF and EKF-5CPF algorithms. Theoretically, the new algorithm has better estimation accuracy and robustness than cubature PF (CPF).

3.1 Fifth-degree cubature particle filter

The 5CPF algorithm combines the latest measurement information of observation stations. During the particle sampling stage, we employ the 5CKF algorithm to determine the mean and covariance for each particle. Then, a new set of particles is selected on the basis of the computed results. The algorithm steps are as follows:

1) Initialization: $k = 0$

$$\bar{\mathbf{X}}_0^{(i)} = E(\mathbf{X}_0^{(i)}) \tag{23}$$

$$\mathbf{P}_0^{(i)} = E\left[(\mathbf{X}_0^{(i)} - \bar{\mathbf{X}}_0^{(i)})(\mathbf{X}_0^{(i)} - \bar{\mathbf{X}}_0^{(i)})^T\right] \tag{24}$$

2) $k = 1, 2, \dots$, and the state and covariance of each particle are calculated using the 5CKF algorithm. According to the Gaussian distribution function of the mean $\mathbf{X}_{k+1}^{(i)}$ and variance $\mathbf{P}_{k+1}^{(i)}$, the updated particle ensemble $(\hat{\mathbf{X}}_{k+1}^{(i)}, \hat{\mathbf{P}}_{k+1}^{(i)})$

is obtained by sampling.

3) Weight updating:

$$\mathbf{Z}^{(i)}(k) = h(\hat{\mathbf{X}}_k^{(i)}) \quad i = 1, 2, \dots, N \tag{25}$$

$$\omega_k'(i) = \frac{1}{\sqrt{2\pi\sigma}} e^{-\frac{(z(k) - Z^{(i)}(k))^2}{2\sigma^2}} \tag{26}$$

$$\bar{\omega}_k'(i) = \frac{\omega_k'(i)}{\sum_{i=1}^N \omega_k'(i)} \tag{27}$$

where $\mathbf{Z}^{(i)}(k)$ is the measurement value of the observation station at the time of k , and σ is the standard deviation, which can be freely selected.

4) Resampling according to $\bar{\omega}'(i)$: The particle set is replicated and eliminated by $\hat{\mathbf{X}}_k^{(i)}$, and the covariance matrix $\mathbf{P}_k^{(i)}$ is updated. Common resampling methods include Random Resample, Multinomial Resample, System Resample, and Residual Resample (Bolić et al., 2004; Kuptamtee and Aunsri, 2022). There is no obvious performance difference between the above resampling methods. Figure 1 describes the algorithm flow of the Random Resample algorithm used in this paper.

5) Normalize the particle weight and weight the output target state.

The essence of the CPF and 5CPF algorithms is to improve the proposed density distribution problem and avoid the blind sampling of particles. However, as the CKF and 5CKF algorithms are limited by the Gaussian model, CPF and 5CPF are only suitable for Gaussian noise systems compared with traditional PF algorithms.

3.2 Mixed-type EKF-5CPF estimator

Although the 5CPF algorithm has a significantly improved filtering performance, the execution time of the PF and 5CKF algorithms is considerably longer compared with

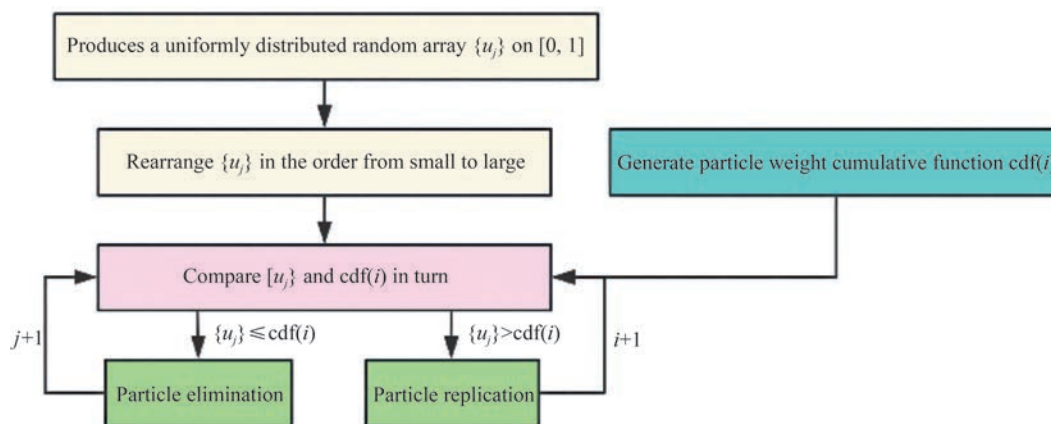


Figure 1 Process of the Random Resample algorithm

those of other algorithms, which greatly reduces the real-time performance of the 5CPF algorithm. Therefore, in actual combat, it is not conducive to achieving rapid attack on a target. Therefore, as shown in Figure 2, we combine EKF with 5CPF. The initial target state prediction computed using the EKF and the covariance matrix replaces the prediction of the target in the 5CPF algorithm, maintaining the high accuracy of the 5CPF while reducing the computational cost of the 5CPF algorithm and improving its robustness. The algorithm steps are as follows:

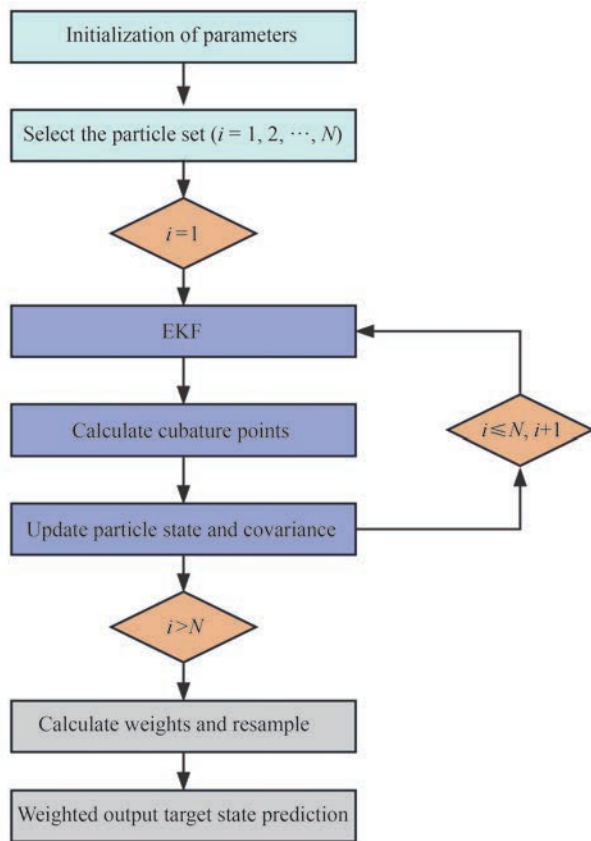


Figure 2 EKF-5CPF algorithm flow

1) Initialize the parameters X_0 , P_0 , R , and Q and extract N initial states according to Equations (23) and (24).

2) Calculate the state forecast and covariance matrix for each particle:

Time update:

$$X'_{k+1|k} = f(\hat{X}_k) \tag{28}$$

$$\hat{P}'_{k+1|k} = \phi_{k+1|k} P_k \phi_{k+1|k}^T + Q_{k+1} \tag{29}$$

$$K'_{k+1} = \hat{P}'_{k+1|k} H_n^T r_1 (H_{k+1} \hat{P}'_{k+1|k} H_{k+1}^T + R_{k+1})^{-1} \tag{30}$$

$$\hat{X}'_k = X'_{k+1} + K'_{k+1} (Z_{k+1} - h(X'_{k+1})) \tag{31}$$

$$\hat{P}'_{k+1} = (I - K'_{k+1} H_{k+1}) \hat{P}'_{k+1|k} \tag{32}$$

Measurement update:

$$S_{k+1} = \text{chol}(\hat{P}'_{k+1})^T \tag{33}$$

$$\hat{X}_{i,k+1|k} = \hat{X}'_{k+1|k} + S_{k+1|k} \gamma_i \tag{34}$$

$$\hat{Z}_{k+1|k}^i = h(\hat{X}_{i,k+1|k}) \tag{35}$$

$$\hat{Z}_{k+1|k} = \omega^i \sum_{i=1}^m \hat{Z}_{k+1|k}^i \tag{36}$$

Iteration is performed according to Equations (12)–(16), and the state and covariance matrix of each particle are output.

3) Sample again according to the particles' state and each covariance matrix, calculate particle weights, resample, and, finally, output the target state.

In this paper, the time update step of the EKF algorithm is combined with the measurement update of the CKF algorithm, which effectively reduces the computational complexity of the 5CPF algorithm and enhances its real-time capabilities.

4 Simulation experiments

The static single-station bearing-only tracking system has partial observability. In practical applications, to accurately track a target, observation stations are usually maneuvered or their number is increased. To further assess the algorithm's performance, this study establishes a bearing-only dual-station system and a single motion station system separately, and analyzes the performance differences of the three algorithms under different conditions.

4.1 Bearings-only tracking system model

We define north and east as the x - and y -axes, respectively. The target azimuth β is the angle between the north and the observation station and the target connection, which is calculated clockwise. The target heading C_w is the angle between the north and the target motion direction.

Figure 3(a) describes the positional relationship between the target and observation in the bearings-only bistatic tracking system, where observation station A is located at (x_0, y_0) , and observation station B is located at (x_1, y_1) . Figure 3(b) displays the relationship between the observation station and the target in the single-motion observation station system. The heading of the observation station is the angle between the north and the motion direction of the observa-

tion platform, which is calculated clockwise. According to Figure 2, the nonlinear representation of this system can be formulated as

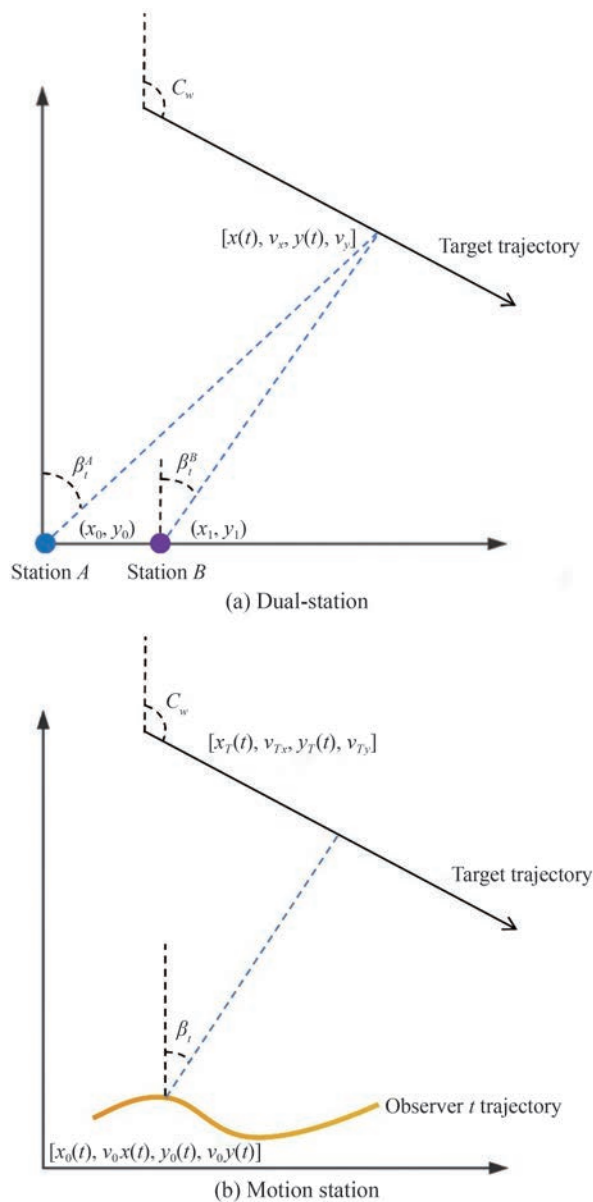


Figure 3 Geometric relationship between the observation station and the target

$$\mathbf{x}(t + T) = \begin{bmatrix} 1 & T & 0 & 0 \\ 0 & 1 & 0 & 0 \\ 0 & 0 & 1 & T \\ 0 & 0 & 0 & 1 \end{bmatrix} \mathbf{x}(t) + \begin{bmatrix} T^2/2 & 0 \\ T & 0 \\ 0 & T^2/2 \\ 0 & T \end{bmatrix} \mathbf{W}(t) \tag{37}$$

$$\mathbf{Z}(t) = \left[\arctan \left(\frac{\mathbf{x}_T(t) - \mathbf{x}_0^{(i)}(t)}{\mathbf{y}_T(t) - \mathbf{y}_0^{(i)}(t)} \right) \right]_{i \times 1} + \mathbf{R}(t) \tag{38}$$

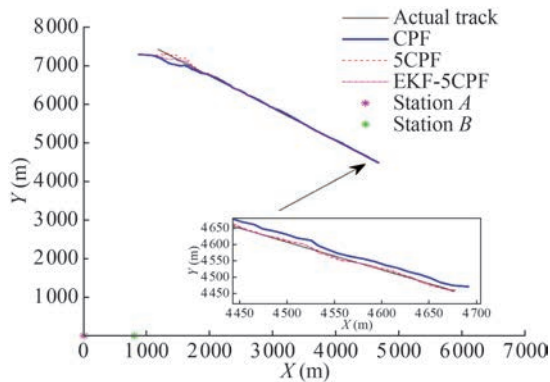
where Equation (37) is the target state equation and Equation (38) is the measurement equation.

4.2 Simulation of bearings-only dual-station

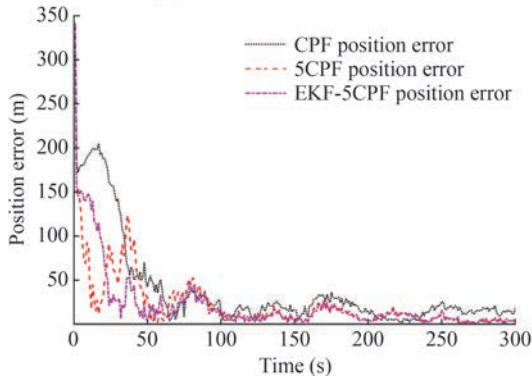
In this paper, we simulate CPF, 5CPF, and EKF-5CPF under different noise environments. The initial distance estimation of the experiment is randomly generated by the Gaussian normal distribution $N(d_0, 200)$, where d_0 represents the true initial distance between the target and station A. We conduct 100 Monte Carlo experiments for each filtering method to analyze the filter performance over the time interval $T = 0 - 300$ s.

In the bearing-only dual-station tracking system, to grant the filter a better tracking effect, the distance between the observation stations can be increased using a towed sonar (generally not more than 1 km). Figures 4 and 5 describe the tracking results, position errors, and velocity errors of CPF, 5CPF, and EKF-5CPF under different observation errors R when the distance between the two observation stations $D = 800$ m. When $R = 0.1$, the three algorithms tend to stabilize after $T = 120$ s, and the estimated error of the position error of the 5CPF and EKF-5CPF algorithms in $t = 260 - 300$ s is reduced to approximately 5 m, but that of CPF is about 20 m (Figure 4(b)). Figure 5(a) displays the estimated trajectories of the three algorithms when $R = 1$. Obviously, as R increases, the three algorithms have different degrees of fluctuation, which reduces their convergence speed and stability. However, the 5CPF and EKF-5CPF algorithms are less affected by noise. As shown in Figure 5(b), although the position root mean square error (RMSE) continues to increase around $t = 200$ s, it quickly decreases to approximately 15 m and remains stable, whereas that of CPF fluctuates greatly, especially in the early stage of filtering. Therefore, compared with the CPF algorithm, the 5CPF and EKF-5CPF algorithms show significant advantages in noise adaptability. Even in high-noise environments, these two algorithms can still converge quickly and maintain good estimation accuracy, showing excellent filtering performance.

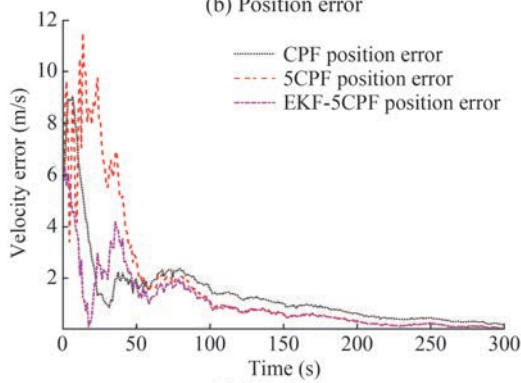
When two sonars are deployed in the bow and stern parts of a ship, the distance between the two stations is close, generally not more than 200 m. Figures 6 and 7 display the tracking performance of CPF, 5CPF, and EKF-5CPF with different observation errors R when the observation station distance $D = 100$ m. The tracking errors of the three algorithms increase with the decrease in the observation station distance. However, the tracking accuracies of 5CPF and EKF-5CPF are generally higher than that of CPF, especially with a large observation error. As shown in Figure 7(b), in the range of 0–300 s, the tracking errors of the three algorithms show a decreasing trend, from the initial 200 m to less than 50 m. However, the accuracies of 5CPF and EKF-5CPF are higher, and the error is approximately 25 m at 300 s.



(a) Actual and estimated tracks

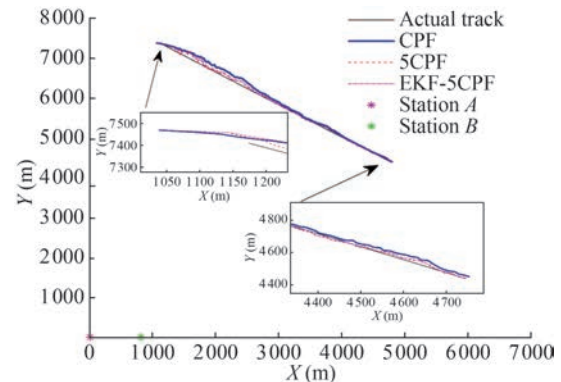


(b) Position error

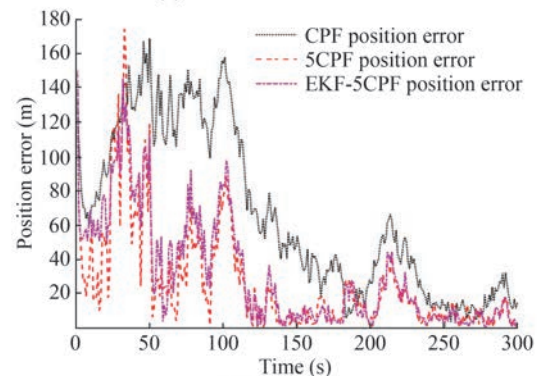


(c) Velocity error

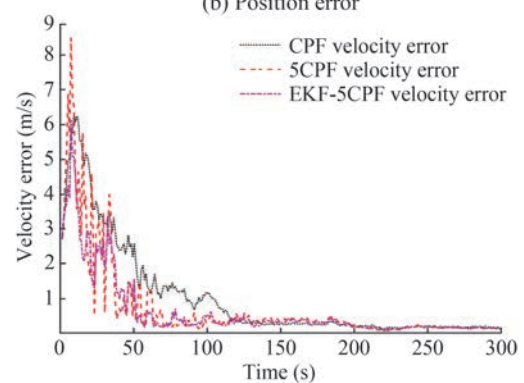
Figure 4 Comparison of the tracking results of three algorithms when $D = 800$ m, $R = 0.1$



(a) Actual and estimated tracks



(b) Position error



(c) Velocity error

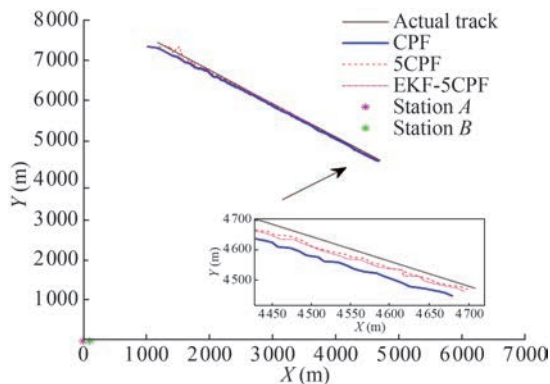
Figure 5 Comparison of the tracking results of three algorithms when $D = 800$ m, $R = 1$

4.3 Simulation of a single-motion station

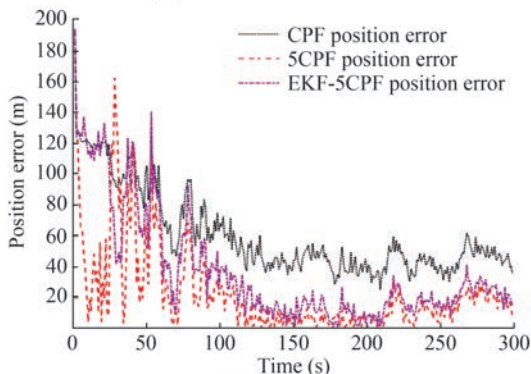
In modern military operations, because of the partial observability of a single station, a target is usually accurately tracked by a submarine or an unmanned underwater vehicle's own maneuvering. Leg-by-leg is the most common maneuver mode, which consists of two straight segments moving at a constant velocity. It is an easy-to-implement maneuver mode that hopes to achieve global optimization in one turn.

In the simulation, the observation station travels at a constant speed of 5 m/s from the coordinate origin, maintaining a direction of 80° . When $t = 150$ s, it turns and the heading is adjusted to 40° . Initially, the target and the obser-

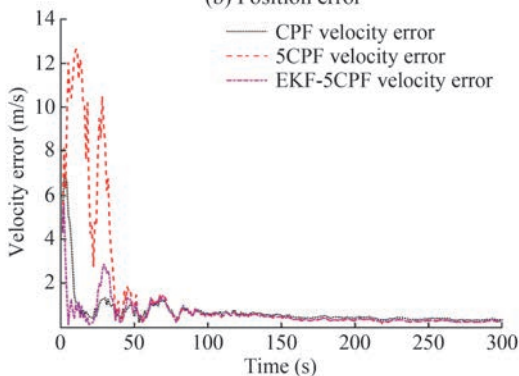
vation station are 5 km apart, and the target travels in a uniform linear motion at a constant speed of 15 m/s and maintains a direction of 130° . Obviously, in Figure 8(a), the target and the observation station move at a large speed difference, causing a huge change in the measurement angle, which is conducive to improving the estimation accuracy. In addition, as the 5CPF and EKF-CPF algorithms use complex cubature point selection rules and increase the number of cubature points, their performance surpasses that of the CPF algorithm throughout the tracking time. Notably, when $t = 50 - 70$ s, the filtering accuracy of the three algorithms is poor (Figure 8(b)). This is because there are inevitably some observable points in the maneuvering process of the observation station. The azimuth measured by the



(a) Actual and estimated tracks



(b) Position error

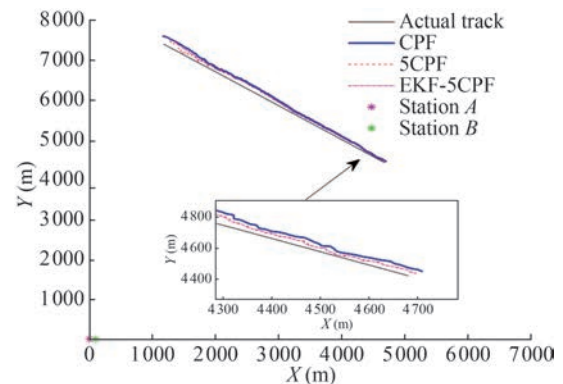


(c) Velocity error

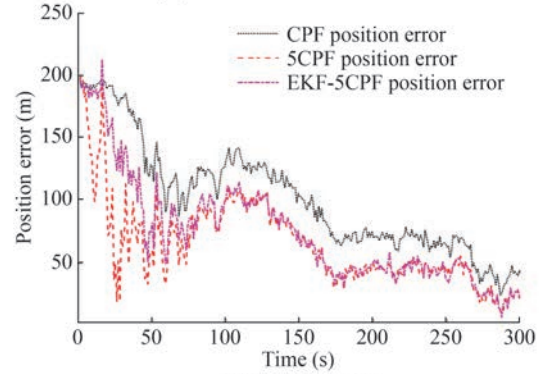
Figure 6 Comparison of the tracking results of three algorithms when $D = 100$ m, $R = 0.1$

observation station at these time points is equivalent to the measurement value of the single static observation station; that is, the movement of the observation station at these time points is invalid.

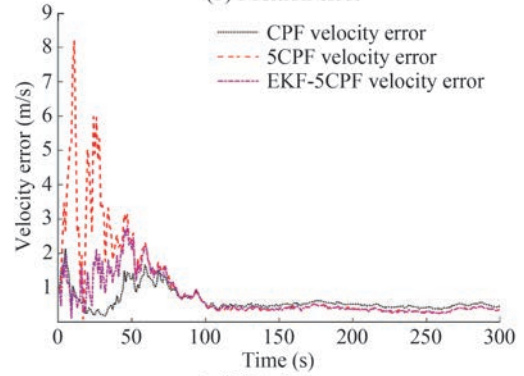
In practical military applications, when the speeds of the target and the observation station are close, it is essential to prolong the tracking time and increase the angle change of the observation station itself to improve the tracking accuracy. Therefore, this study simulates the tracking results of the three algorithms when the observation station is doing a circular motion with a radius of 500 m and a speed of about 5 m/s when $T = 1200$ s (Figure 9). Figure 9(b) describes the estimated position RMSE of the filter. Obviously, the 5CPF algorithm and the EKF-5CPF algorithm



(a) Actual and estimated tracks



(b) Position error



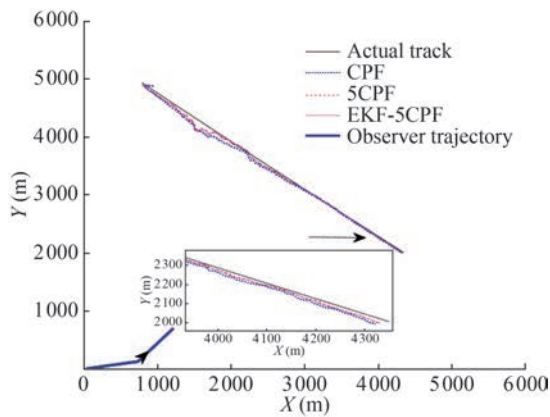
(c) Velocity error

Figure 7 Comparison of the tracking results of three algorithms when $D = 100$ m, $R = 1$

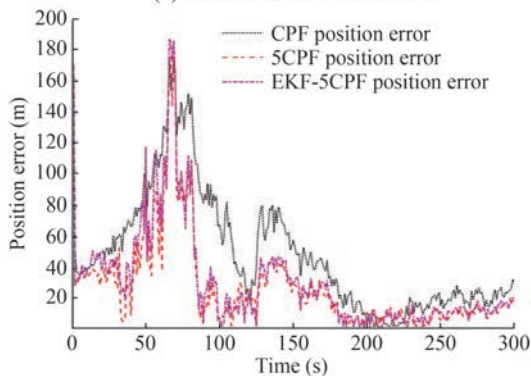
have faster convergence speeds and higher convergence accuracies than the CPF algorithm. Notably, when $t = 0 - 480$ s, the position error of 5CPF and EKF-5CPF is about 100 m lower than that of CPF.

4.4 Running time and global error

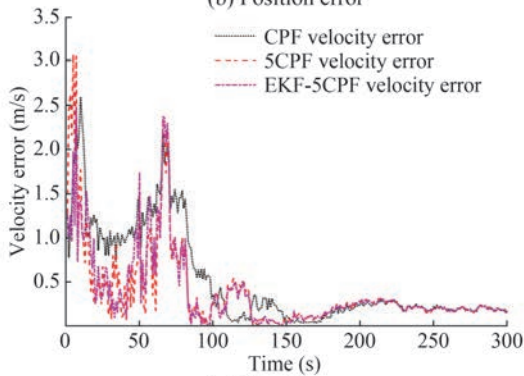
In this part, this paper first simulates the running time of CPF, 5CPF, and EKF-5CPF with different particle numbers and compares their computational complexities. For most target tracking studies, traditional error evaluation methods are limited to assessing the tracking performance of filters at individual time points rather than evaluating the overall effectiveness of the target tracking process. This paper introduces global error as a metric (Lu et al., 2022). This



(a) Actual and estimated tracks



(b) Position error



(c) Velocity error

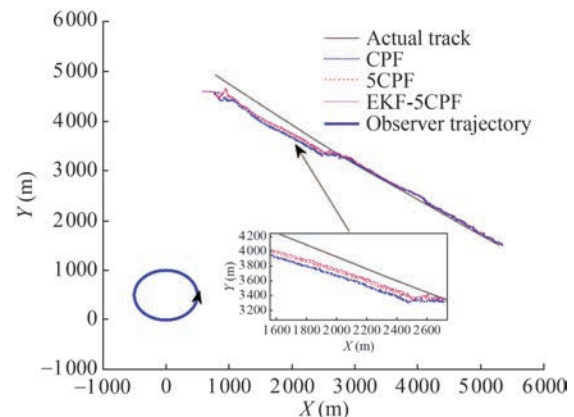
Figure 8 Leg-by-leg maneuver of the observer

approach aims to comprehensively assess the overall effectiveness of the tracking algorithm throughout its entire cycle. Using this method, we can accurately evaluate algorithms that may not show significant, immediate error optimization during the tracking process but still contribute to substantial improvements in the overall tracking results. Its equation is as follows:

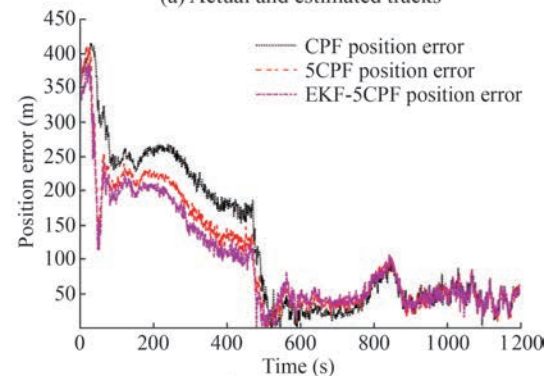
$$E = \pm \sqrt{\frac{\sum_{k=1}^M [(\hat{x}_k - x_k)^2 + (\hat{y}_k - y_k)^2]}{2M}} \quad (39)$$

where, (\hat{x}_k, \hat{y}_k) is the predicted position. (x_k, y_k) is the actual location of the target.

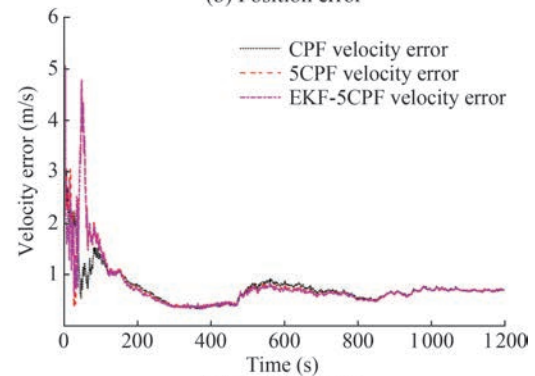
For a uniform linear moving target, the 5CPF algorithm



(a) Actual and estimated tracks



(b) Position error



(c) Velocity error

Figure 9 Circular maneuver of the observer

selects 33 cubature points near each particle, whereas the CPF algorithm only selects eight cubature points. Therefore, as the number of particles increases, the calculation amounts of EKF-5CPF and 5CPF algorithms increase exponentially, and the real-time performance of these algorithms declines (Figure 10). When $N = 200$ and $t = 300$ s, the calculation amount and calculation time are much higher than those of the CPF algorithm. The EKF-5CPF algorithm uses the EKF algorithm to replace the 5CPF algorithm when the time of each particle is updated, which effectively reduces the calculation amount of the 5CPF algorithm. Through ten Monte Carlo experiments, CPF's running time is approximately 3–5 s, that of 5CPF is about 15–18 s, surpassing that of CPF significantly, and that of EKF-5CPF is about

11 s (Figure 11). Although the running time of 5CPF is still higher than that of CPF, it reduces the calculation time of 5CPF to a certain extent and enhances the algorithm’s real-time capability.

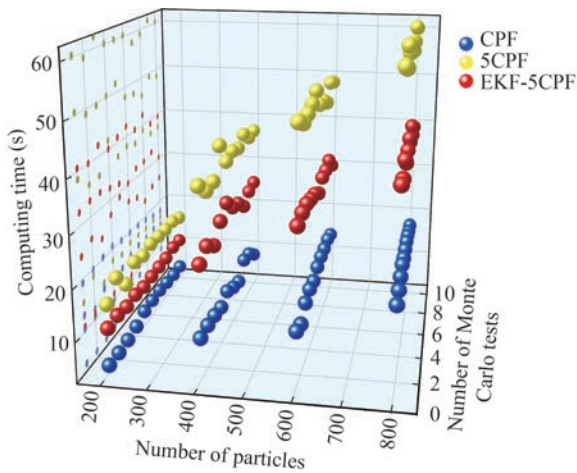


Figure 10 Comparison of the amounts of calculation as the particle count rises

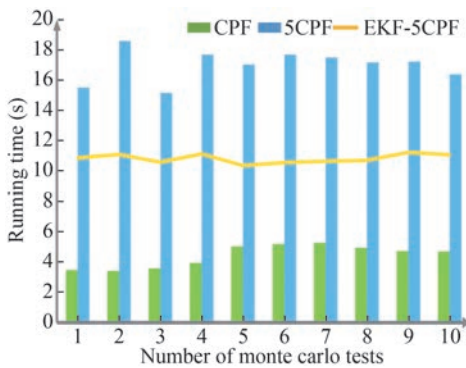


Figure 11 Comparison of calculation times when $N = 200$

Table 1 describes the global errors of EPF, UPF, CPF, 5CPF, and EKF-5CPF in different noise environments. Obviously, the three algorithms are sensitive to noise, but 5CPF and EKF-5CPF have better robustness. As the observation noise R increases, the mean square error increases slowly compared with those of the traditional algorithms and the performance advantage becomes more apparent. In addition, the EKF-5CPF algorithm shows better tracking accuracy than the 5CPF algorithm in a low-noise environment.

Table 1 Global errors in different observations

Errors	$R = 0.1$	$R = 0.5$	$R = 1$	$R = 2$
E_{EPF} (m)	±46.842	±56.965	±106.210	±222.430
E_{UPF} (m)	±12.551	±21.445	±49.747	±65.401
E_{CPF} (m)	±13.251	±20.260	±24.026	±37.276
E_{5CPF} (m)	±9.064	±13.223	±15.100	±27.492
$E_{EKF-5CPF}$ (m)	±7.708	±11.984	±13.509	±28.144

Table 2 lists the global errors of the three algorithms based on different observatory trajectories. Overall, the errors of 5CPF and EKF-5CPF are less than those of CPF, and the filtering accuracy is enhanced. When the target velocity is close to that of the observation station, the estimation error of the leg-by-leg motion is large, which cannot meet the high-precision requirements of the application. Other motion modes, such as sinusoidal motion, circular motion, and spiral motion, change greatly due to the angle of the observation station itself, leading to a large change in the angle measurement value of the observation station and thus allowing for a better filter working performance.

Table 2 Global errors in different observatory trajectories

Errors	Leg-by-leg	Sinusoidal motion	Circular motion	Screw motion
E_{CPF} (m)	±231.412	±50.3270	±30.120	±28.989
E_{5CPF} (m)	±143.195	±38.7368	±28.502	±26.451
$E_{EKF-5CPF}$ (m)	±130.305	±35.1070	±28.751	±25.450

5 Conclusions

In this study, we combine 5CKF with PF and propose the 5CPF algorithm with better performance. However, because of high precision of 5CPF is realized with increased calculation amount and time, the algorithm exhibits poor real-time performance, which is not conducive to the rapid attack of a target in actual combat. Therefore, we propose a new EKF-5CPF algorithm that maintains the excellent performance of the 5CPF algorithm while effectively reducing the filtering time, which is of great significance for actual military operations.

In addition, the bearings-only dual-station system model and the single-motion station model are established, and three algorithms are simulated multiple times under different scenarios and different noise environments. The following conclusions are drawn:

a) Compared with CKF, 5CPF has more obvious advantages in tracking accuracy, convergence speed, and algorithm stability. Particularly in scenarios characterized by close proximity to the observation station and elevated noise levels, the 5CPF algorithm integrates a larger number of cubature points and employs more sophisticated calculation rules. Moreover, it estimates the target state by assigning weights to each cubature point rather than relying on a simple average of these points. Consequently, it demonstrates enhanced robustness and adaptability across varying noise environments.

b) As the quantity of particles grows, the computational burden of the 5CPF algorithm rises considerably, resulting in operation times that are considerably longer than those of the CPF algorithm. The EKF-5CPF algorithm effec-

tively mitigates the computational complexity associated with the 5CPF algorithm, thereby enhancing its real-time performance.

c) When the observation error R is minimal, the EKF-5CPF algorithm has better filtering performance than the 5CPF algorithm. As R increases, the performance of EKF-5CPF decreases faster than that of 5CPF, but it is still far better than that of CPF.

d) In the single-motion station system, the movement mode of the observation station has a notable influence on the accuracy of tracking. The invalid observation station maneuver impacts the filter's performance and compromises its stability. When the observation station is close to the target speed, it still cannot meet the actual combat requirements if only a simple leg-by-leg motion is performed, although the tracking errors of both the 5CPF and EKF-5CPF algorithms are markedly lower than that of CPF. Therefore, the observation station should make its own course change faster circular motion or other more complex motion to achieve high-precision and high real-time tracking of the target.

Funding Supported by the Guangxi Special Program for Technological Innovation Guidance (No. GuiKeAC25069006).

Competing interest Yaan Li is an editorial board member for the Journal of Marine Science and Application and was not involved in the editorial review, or the decision to publish this article. All authors declare that there are no other competing interests.

References

- Arasaratnam I, Haykin SS (2009) Cubature Kalman filters. *IEEE Transactions on Automatic Control* 54(6): 1254-1269. <https://doi.org/10.1109/TAC.2009.2019800>
- Arulampalam MS, Maskell S, Gordon N, Clapp T (2002) A tutorial on particle filters for online nonlinear/non-Gaussian Bayesian tracking. *IEEE Transactions on Signal Processing* 50(2): 174-188. <https://doi.org/10.1109/78.978374>
- Arulampalam S, Ristic B (2000) Comparison of the particle filter with range-parameterized and modified polar EKFs for angle-only tracking. *Signal and Data Processing of Small Targets Bellingham: SPIM 4048*: 288-299. <https://doi.org/10.1117/12.391985>
- Badrials L, Arulampalam S, Nguyen NH, Finn A (2020) An algebraic closed-Form solution for bearings-only maneuvering target motion analysis from a nonmaneuvering platform. *IEEE Transactions on Signal Processing* 68: 4672-4687. <https://doi.org/10.1109/TSP.2020.3012004>
- Bolić M, Djurić PM, Hong S (2004) Resampling algorithms for particle filters: A computational complexity perspective. *EURASIP Journal on Advances in Signal Processing* Article number: 403686. <https://doi.org/10.1155/S1110865704405149>
- Divya KS, Ramesh KS, Rao SK, Naga Divya G (2021) Underwater object tracking using unscented Kalman filter. 2021 3rd International Conference on Advances in Computing, Communication Control and Networking (ICAC3N). Piscataway: IEEE 1729-1733. <https://doi.org/10.1109/ICAC3N53548.2021.9725674>
- Farina A (1999) Target tracking with bearings-Only measurements. *Signal Processing* 78(1): 61-78. [https://doi.org/10.1016/S0165-1684\(99\)00047-X](https://doi.org/10.1016/S0165-1684(99)00047-X)
- Gao B, Xu D, Yan W (2010) Framed-quadtrees path planning for an underwater vehicle with the task of tracking a moving target. *Journal of Marine Science and Application* 9: 27-33. <https://doi.org/10.1007/s11804-010-8011-6>
- Hammersley JM, Morton KW (1954) Poor man's Monte Carlo. *Journal of the Royal Statistical Society Series B(Methodological)* 16: 23-38. <https://doi.org/10.1111/j.2517-6161.1954.tb00145.x>
- Havangi R (2018) Target tracking with unknown noise statistics based on intelligent H-infinity particle filter. *International Journal of Adaptive Control and Signal Processing* 32: 858-874. <https://doi.org/10.1002/acs.2872>
- Jia B, Xin M, Cheng Y (2013) High-degree cubature Kalman filter. *Automatica* 49(2): 510-518. <https://doi.org/10.1016/j.automatica.2012.11.014>
- Jia B, Xin M, Cheng Y (2012) The high-degree cubature Kalman filter. 2012 IEEE 51st IEEE Conference on Decision and Control (CDC). Piscataway: IEEE 4095-4100. <https://doi.org/10.1109/CDC.2012.6426413>
- Kotecha JH, Djurić PM (2003) Gaussian particle filtering. *IEEE Transactions on Signal Processing* 51(10): 2592-2601. <https://doi.org/10.1109/TSP.2003.816758>
- Kulikova MV, Kulikov GY (2021) MATLAB-based general approach for square-root extended-unscented and fifth-degree cubature Kalman filtering methods. *European Journal of Control* 59: 1-12. <https://doi.org/10.1016/j.ejcon.2021.01.003>
- Kumar DVANR, Rao SK, Raju KP (2016) Integrated unscented Kalman filter for underwater passive target tracking with towed array measurements. *Optik* 127(5): 2840-2847. <https://doi.org/10.1016/j.ijleo.2015.11.217>
- Kuptamete C, Aunsri N (2022) A review of resampling techniques in particle filtering framework. *Measurement* 193: 110836. <https://doi.org/10.1016/j.measurement.2022.110836>
- Li T, Villarubia G, Sun S, Corchado JM, Bajo J (2015) Resampling methods for particle filtering: Identical distribution, a new method, and comparable study. *Frontiers of Information Technology & Electronic Engineering* 16: 969-984. <https://doi.org/10.1631/FITEE.1500199>
- Li Y, Zhao Z (2019) Passive tracking of underwater targets using dual observation stations. 2019 16th International Bhurban Conference on Applied Sciences and Technology (IBCAST). Piscataway: IEEE 867-872. <https://doi.org/10.1109/IBCAST.2019.8667211>
- Lu X, Li F, Tang J, Chai Z, Hu M (2022) A new performance index for measuring the effect of single target tracking with Kalman particle filter. *International Journal of Modern Physics C* 33(9): 2250116. <https://doi.org/10.1142/S0129183122501169>
- Mu J, Tian F, Cheng J (2024) Adaptive and robust fractional gain based interpolatory cubature Kalman filter. *Measurement and Control* 57(4): 428-442. <https://doi.org/10.1177/00202940231200954>
- Nardone S, Lindgren A, Gong K (1984) Fundamental properties and performance of conventional bearings-only target motion analysis. *IEEE Transactions on Automatic Control* 29(9): 775-787. <https://doi.org/10.1109/TAC.1984.1103664>
- Pillon D, Perez-Pignol AC, Jauffret C (2016) Observability: Range-only vs. bearings-only target motion analysis for a leg-by-leg observer's trajectory. *IEEE Transactions on Aerospace and Electronic Systems* 52(4): 1667-1678. <https://doi.org/10.1109/TAES.2016.150016>
- Shen Y, Li Y, Li W, Gao H, Wu C (2024a) A novel underwater weak target detection method based on 3D chaotic system and maximal

- overlap discrete wavelet transform. *The European Physical Journal Plus* 139: 325. <https://doi.org/10.1140/epjp/s13360-024-05135-w>
- Shen Y, Li Y, Li W, Gao H, Wu C (2024b) A novel underwater weak signal detection method based on parameter optimized VMD and 3D chaotic system. *Digital Signal Processing* 151: 104571. <https://doi.org/10.1016/j.dsp.2024.104571>
- Shen Y, Li Y, Li W, Yao Q (2024c) Generalized fined-grained multiscale information entropy with multi-feature extraction and its application in phase space reconstruction. *Chaos, Solitons & Fractals* 189(part 2): 115710. <https://doi.org/10.1016/j.chaos.2024.115710>
- Shen Y, Li Y, Li W, Yao Q, Gao H (2025) Extremely multi-stable grid-scroll memristive chaotic system with omni-directional extended attractors and application of weak signal detection. *Chaos, Solitons & Fractals* 190: 115791. <https://doi.org/10.1016/j.chaos.2024.115791>
- Singh AK, Bhaumik S (2015) Higher degree cubature quadrature kalman filter. *International Journal of Control, Automation and Systems* 13: 1097-1105. <https://doi.org/10.1007/s12555-014-0228-8>
- van der Merwe R, Doucet A, de Freitas N, Wan E (2000) The unscented particle filter. *Advances in Neural Information Processing Systems* 13 (NIPS 2000). Cambridge: Cambridge University Technical Report CUED/F-INFENG/TR 380
- Wang S, Feng J, Tse CK (2014) Spherical simplex-radial cubature Kalman filter. *IEEE Signal Processing Letters* 21: 43-46. <https://doi.org/10.1109/LSP.2013.2290381>
- Weiss H, Moore J (1980) Improved extended Kalman filter design for passive tracking. *IEEE Transactions on Automatic Control* 25(4): 807-811. <https://doi.org/10.1109/TAC.1980.1102436>
- Xu B, Wang Z (2006) A new algorithm of bearings-only multi-target tracking of bistatic system. *Journal of Control Theory and Applications* 4: 331-337. <https://doi.org/10.1007/s11768-006-5320-z>
- Zhang X, Liu D, Yang Y, Liang J (2021) An intelligent particle filter with adaptive M-H resampling for liquid-level estimation during silicon crystal growth. *IEEE Transactions on Instrumentation and Measurement* 70: 1-12. <https://doi.org/10.1109/TIM.2020.3026760>
- Zhu J, Liu B, Wang H, Li Z, Zhang Z (2020) State estimation based on improved cubature Kalman filter algorithm. *IET Science, Measurement & Technology* 14: 536-542. <https://doi.org/10.1049/iet-smt.2019.0363>